

# White light emission from an exciplex based on a phosphine oxide type electron transport compound in a bilayer device structure†

Cite this: DOI: 10.1039/c3ra43017k

Yan Zhao, Lian Duan,\* Xiao Zhang, Deqiang Zhang, Juan Qiao, Guifang Dong, Liduo Wang and Yong Qiu\*

A white organic light emitting diode (OLED) with a simple structure using exciplex emission is fabricated. The white emission of exciplex is formed at the interface between new electron transport material anthracene-9,10-diylbis(diphenylphosphine oxide) (DPPA) and hole transporting layer *N,N'*-bis(naphthalen-1-yl)-*N,N'*-bis(phenyl)benzidine (NPB). Pure white emission with Commission International de L'Eclairage (CIE) coordinates (0.33, 0.33) at the equal-energy white point is obtained. The phosphine oxide type material DPPA based OLEDs work well when Al is directly deposited on them, without an electron injection layer. In order to investigate the mechanism of electron injection from Al to DPPA, X-ray photoelectron spectroscopy (XPS) measurements have been carried out and revealed that the improved electron injection is due to the existence of interaction between the phosphine oxide group of DPPA and Al at the DPPA/Al interface.

Received 17th June 2013

Accepted 9th September 2013

DOI: 10.1039/c3ra43017k

[www.rsc.org/advances](http://www.rsc.org/advances)

## Introduction

Since the great development of organic light emitting diodes (OLEDs) due to the advantages of wide viewing angle, high-efficiency, self-emission, and low driving voltage,<sup>1–3</sup> white OLEDs (WOLEDs) have achieved more attention for applications in solid state light sources, flat-panel displays and even flexible displays. For efficient WOLEDs, multi-emission layers or stacked emission layers are necessary to optimize the performance.<sup>4–7</sup> As to the structure of multi-emission layers or stacked emission layers device, their complicated fabrication and high cost process may be a great challenge for business application. In order to minimize the structure of the WOLEDs, many solutions can be introduced, such as a single-emitting-compound,<sup>8</sup> exciplexes<sup>9</sup> or electroplexes.<sup>10</sup> For the exciplex, it is happened between different molecules in the excited state of the donor to the acceptor in the ground state, and from the emission of exciplex, it can be observed both in electroluminescence (EL) and photoluminescence (PL) spectrum.<sup>11</sup> For the electroplex, it is formed between the lowest unoccupied molecular orbital (LUMO) of electron transport material and the highest occupied molecular orbital (HOMO) of hole transport material, while from the emission of electroplex, it can be observed only in EL spectrum

not in PL spectrum.<sup>12,13</sup> Exciplex and electroplex can be used to simplify the structure of WOLEDs.

In this letter, a white OLED using exciplex emission is demonstrated. Although the photoluminescent properties of the electron transporting material anthracene-9,10-diylbis(diphenylphosphine oxide) (DPPA) have been reported,<sup>14</sup> its electronic and optoelectronic properties have not been investigated. In this work, DPPA is a multi-functional material in OLED. It is used not only as an emission material to emit blue light, but also as a electron transport material with high electron mobility in OLED. The white emissions of exciplex is formed at the interface DPPA and the hole transporting layer *N,N'*-bis(naphthalen-1-yl)-*N,N'*-bis(phenyl)benzidine (NPB), and a fairly pure white emission at the equal-energy white point with Commission International de L'Eclairage (CIE) coordinates (0.33, 0.33) is obtained. We also develop a white OLED with the structure of using the phosphine oxide type material DPPA layer on which Al is following directly deposited, without an electron injection layer, exhibiting the efficient electron injection. In order to investigate the mechanism of electron injection from Al to DPPA layer, X-ray photoelectron spectroscopy (XPS) is carried out. It is found that the existence of interaction between the phosphine oxide group of DPPA and Al at the DPPA/Al interface is the main reason for the efficient electron injection.

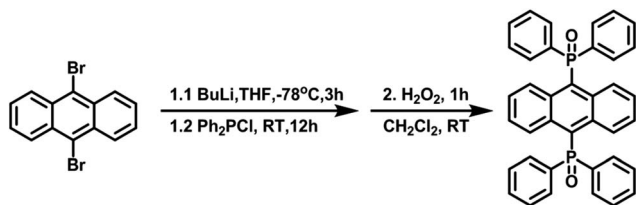
## Results and discussion

### Synthesis and characterization

The synthesis route and chemical structure of DPPA are shown in Scheme 1, which has some modifications with previous

Key Lab of Organic Optoelectronics and Molecular Engineering of Ministry of Education, Department of Chemistry, Tsinghua University, Beijing 100084, China. E-mail: duanl@mail.tsinghua.edu.cn; qiuy@mail.tsinghua.edu.cn; Fax: +86 10 62795137; Tel: +86 10 62788802

† CCDC 958068. For crystallographic data in CIF or other electronic format see DOI: 10.1039/c3ra43017k



**Scheme 1** Synthetic route toward DPPA.

reports.<sup>14</sup> 9,10-Dibromoanthracene (2.0 g, 6 mmol) was added to a dried 150 mL flask followed by adding 60 mL distilled THF to form a suspension under nitrogen. The reaction mixture was cooled to  $-78\text{ }^{\circ}\text{C}$  and then *n*-BuLi (24 mmol) was added dropwise over 2 h. The suspension was stirred at room temperature for another 12 h after adding  $\text{PPh}_2\text{Cl}$  (5.3 g, 24 mmol). 5 mL methanol was added to reaction mixture to quench the reaction and filtrated to collect the yellow solid. 15 mL 30%  $\text{H}_2\text{O}_2$  solution was added to a suspension of the yellow precipitate in methylene chloride (50 mL). The reaction mixture was stirred for 1 h and the organic layer was wash by 30 mL water for 2 times. The crude product was purified by silica column with methylene chloride–acetone (5 : 1). Yellow-green 9,10-bis(diphenylphosphoryl)anthracene (DPPA) was obtained with a yield of 61%. The compound was purified using the silica column method with further purification by sublimation, producing very pure powders.  $^1\text{H}$  NMR (600 MHz,  $\text{CDCl}_3\text{-d}_1$ ): 8.53 (s, 4H), 7.78 (d,  $J = 7.2$  Hz, 4H), 7.74 (d,  $J = 7.5$  Hz, 4H), 7.58 (d,  $J = 7.2$  Hz, 4H), 7.51 (d,  $J = 5.4$  Hz, 4H), 7.31 (s, 4H), 7.17 (s, 4H); elemental analysis calcd for  $\text{C}_{38}\text{H}_{28}\text{P}_2\text{O}_2$ : C 78.88, H 4.88, O 5.53; found: C 78.92, H 4.65, O 5.79%.

The molecular structure of DPPA was further determined by single-crystal X-ray crystallographic analysis, as shown in Fig. 1. The dihedral angles of benzene–naphthalene were  $85$  and  $55^{\circ}$ , respectively. Single crystals of DPPA were grown from recrystallization of methylene chloride solution during heating. The room temperature single-crystal X-ray experiments were performed on a RIGAKU SATURN 724 + CCD diffractometer equipped with a graphite monochromatized  $\text{Mo K}\alpha$  radiation. The structure was solved by direct methods and refined with a full-matrix least-squares technique based on  $F^2$  with the SHELXL-97 crystallographic software package. Selected crystal data of DPPA: space group  $P2_1/n$  with  $a = 7.87\text{ \AA}$ ,  $b = 12.00\text{ \AA}$ ,  $c = 14.80\text{ \AA}$ ,  $\alpha = 90^{\circ}$ ,  $\beta = 94.7^{\circ}$ ,  $\gamma = 90^{\circ}$ .

### Thermal properties

Thermal gravimetric analysis (TGA) and differential scanning calorimetry (DSC) were carried out to measure the thermal stability. As shown in Fig. 2, the decomposition temperature ( $T_d$ ) of compound DPPA was  $339\text{ }^{\circ}\text{C}$  under nitrogen at the heating rate of  $10\text{ }^{\circ}\text{C min}^{-1}$ . In the first DSC scan, an endothermic peak appeared at  $265\text{ }^{\circ}\text{C}$ , corresponding to the melting point ( $T_m$ ) of DPPA. After quenched by liquid nitrogen, the second DSC scan was measured and the glass transition temperature ( $T_g$ ) of DPPA was  $108\text{ }^{\circ}\text{C}$ .

### Photophysical properties

The UV-vis absorption and photoluminescence (PL) spectrum of DPPA in methylene chloride were measured, as shown in Fig. 3. The absorption edge of UV-vis spectrum is about 448 nm, indicating that the energy gap of DPPA is 2.8 eV. The

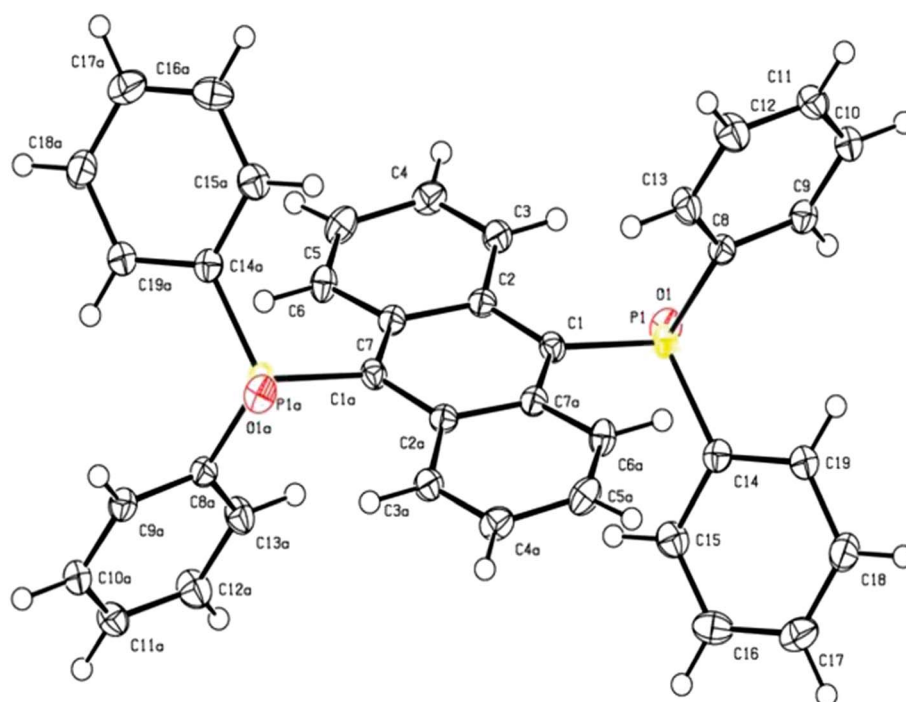


**Fig. 1** The single crystal structure of DPPA.

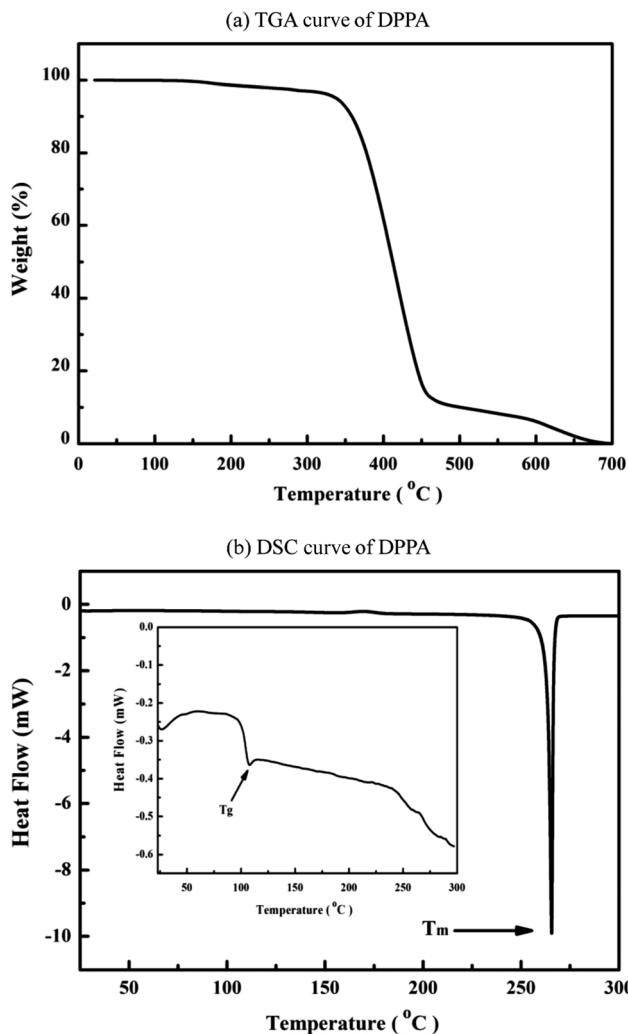


Fig. 2 TGA and DSC curves of DPPA recorded at a heating rate of  $10\text{ }^{\circ}\text{C min}^{-1}$ .

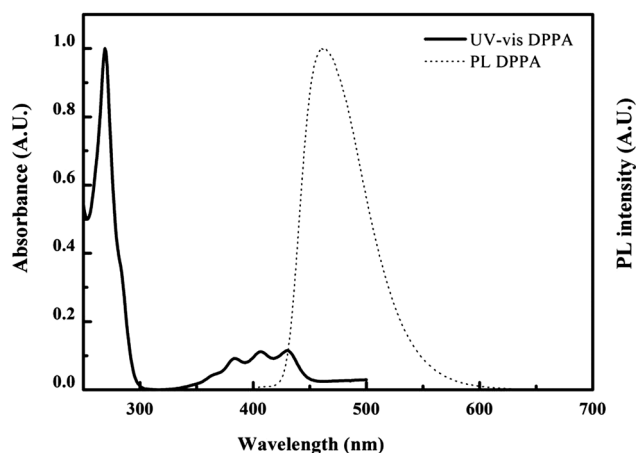


Fig. 3 UV-vis absorption and photoluminescence spectrum of DPPA in methylene chloride solution.

PL emission peak of DPPA in the methylene chloride is observed at 462 nm. The quantum efficiency of DPPA thin film is 5.5%.

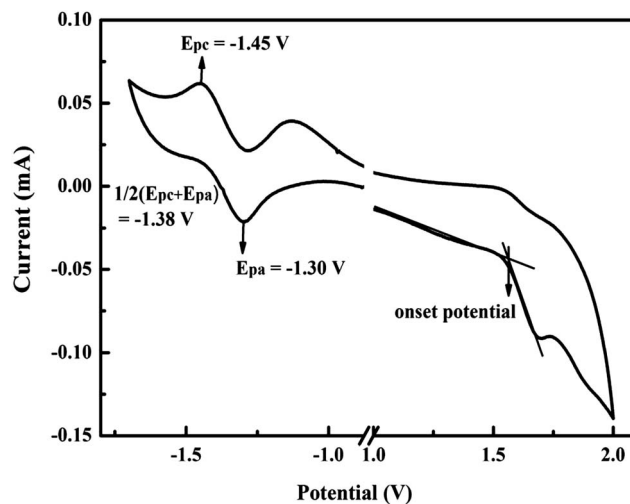


Fig. 4 The cyclic voltammogram for DPPA.

### The cyclic voltammogram measurement

The cyclic voltammograms (CV) were measured in dichloromethane to study the energy levels of DPPA. The highest occupied and lowest unoccupied molecular orbital (HOMO/LUMO) energy levels can be calculated from the CV measurement data together with the UV-vis absorption spectrum. From the CV measurement shown in Fig. 4, the HOMO energy level of DPPA is determined to be 5.9 eV, while the LUMO energy level is calculated from the HOMO level and the  $E_g$  (2.8 eV, calculated from the UV-vis absorption spectrum) to be 3.1 eV.

### Quantum chemical calculations

Density functional theory (DFT) calculations on the ground state of DPPA were carried out at the B3LYP/6-31G(d) level. The structure was first optimized from the geometry in single crystal. All calculations were performed with Gaussian 09 software package, as shown in Fig. 5.

### Electron mobility

We also measured the electron mobility of DPPA. The structure of the device is ITO/DPPA ( $2\text{ }\mu\text{m}$ )/Mg:Ag (150 nm). A nitrogen pulsed laser was used as the excitation light source, which is directed from the ITO side to generate a thin sheet of excess carriers near the ITO/organic interface. The transient photocurrent signals were recorded by a digital storage oscilloscope. The transient current is shown in Fig. 6. The transit time was extracted from the double-logarithmic plot of the transient photocurrent. The charge mobility  $\mu$  could be calculated as:<sup>15</sup>

$$\mu = L^2/t_{\tau}V.$$

Where  $L$  is the film thickness,  $t_{\tau}$  is the transit time, and  $V$  is the applied electric field. Fig. 6 shows the electron mobility of DPPA at different electric fields. The negative field dependence may be attributed to the large positional disorder.<sup>16</sup>

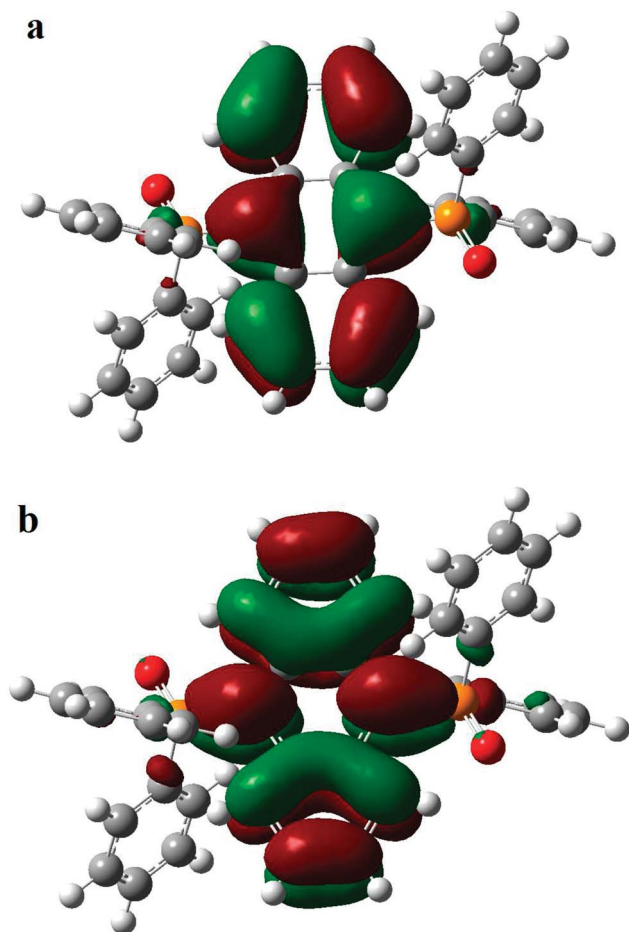


**Fig. 5** Isocontour plots of HOMO and LUMO wavefunctions of DPPA obtained at the: B3LYP/6-31G(D) level. (a) HOMO orbital of DPPA. (b) LUMO orbital of DPPA. All the MO surfaces correspond to an isocontour value of  $|\psi| = 0.025$  a.u.

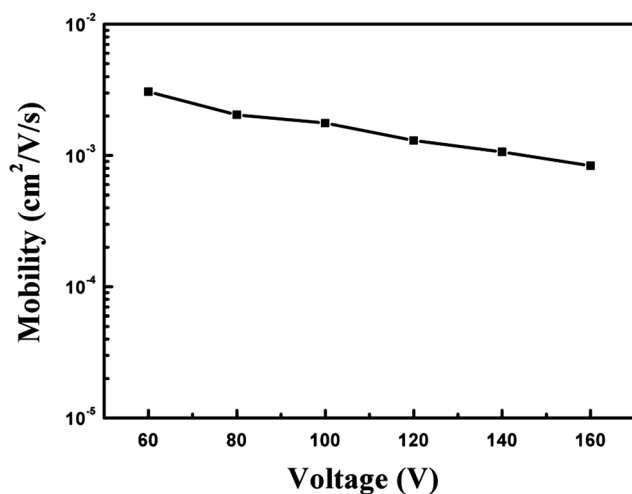


**Fig. 6** The electron mobility of DPPA at different electric fields under the structure of ITO/DPPA (2  $\mu$ m)/Mg:Ag (150 nm).

Ag(50 nm)	Al(120 nm)
Mg: Ag(150 nm)	DPPA(50 nm)
DPPA(50 nm)	NPB(50 nm)
NPB(50 nm)	ITO
ITO	ITO
Glass Substrate	Glass Substrate

Device A

Device B

**Fig. 7** The structures for the white OLED devices Device A and Device B.

### Electroluminescent properties

As shown in Fig. 7, two series of devices were fabricated to obtain white OLEDs. These are Device A, with a structure of ITO/NPB (50 nm)/DPPA (50 nm)/Mg:Ag (150 nm)/Ag (50 nm), and Device B, with a structure of ITO/NPB (50 nm)/DPPA (50 nm)/Al (120 nm). The thickness of these materials was measured by the scanning probe microscope system-atomic force microscope (AFM). The luminance-current characteristics of devices were measured using a PR705 spectroscan spectrometer and the brightness-voltage ( $B$ - $V$ ) characteristics were measured by a Keithley 4200 semiconductor characterization system and calibrated silicon. PL spectra were recorded with a fluoro-spectrophotometer (Jobin Yvon, FluoroMax-3).

The EL spectrum of the above mentioned devices were shown in Fig. 8, and the PL spectrum for the thin films of DPPA, NPB and DPPA:NPB (1 : 1) on quartz glass substrate. For Device A, the device exhibited a white EL spectrum with peaks at 486 and 662 nm, and as shown in Fig. 8(b), a fairly pure white emission with CIE coordinates (0.33, 0.33) at the equal-energy white point was exhibited. The emission with peak at 486 nm in the blue region was corresponding well to the PL spectrum of DPPA with peak at 482 nm, apparently generated from the singlet excited state of the DPPA molecule in the DPPA layer. Because NPB is a hole transport material and also provides an electron block effect, most excitons will be accumulated in the DPPA layer near the interface with NPB. The emission in the long wavelength region with a peak at 662 nm was observed in EL spectrum, red shifted comparing with the emission of the exciplex peak at 620 nm in the PL spectrum of the DPPA:NPB (1 : 1) thin film. This phenomenon indicated that the white EL spectrum of the devices seem be originated from the exciplex formed at the interface DPPA and NPB.

The red-shift is attributed to the possible electroplex (donor<sup>+</sup>/acceptor<sup>-</sup>)\* formed at the DPPA/NPB interface, as the columbic interaction is stronger in the electroplex than in the exciplex.<sup>17-19</sup> The emission of exciplex or would obey the relationship as follows:

$$h\nu_{\max} = I_D - A_A - E_c$$

$$E_c = e^2/4\pi\epsilon_0\epsilon r_c$$

where  $I_D$  is the ionization potential of the donor,  $A_A$  is the electron affinity of the acceptor and  $E_c$  is the columbic attraction energy between the ions situated at a distance  $r_c$ .<sup>20,21</sup>

The ionization potential of the donor (NPB) is 5.4 eV, and the electron affinity of the acceptor (DPPA) is 3.1 eV. As to  $h\nu_{\max} = I_D$

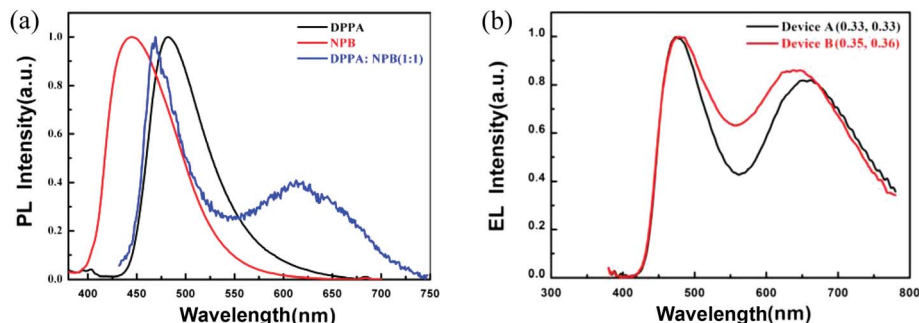


**Fig. 8** (a) PL spectra of DPPA, NPB and DPPA:NPB (1 : 1) thin films on quartz glass substrate, (b) EL spectra of white OLEDs Device A and Device B. Device A: ITO/NPB/DPPA/Mg:Ag/Ag, Device B: ITO/NPB/DPPA/Al.

$-A_A - E_c = 5.4 \text{ eV} - 3.1 \text{ eV} - E_c$ . For the 662 emission,  $h\nu_{\text{max}}$  is about 1.9 eV that related to  $E_c = 0.4 \text{ eV}$ . Then an  $\epsilon$  value is close to 2.6–3 for organic films,<sup>21,22</sup> and we get a distance between ions  $r_c$  around 1.2–1.4 nm. Stable exciplexes can be formed at distances below 0.4 nm,<sup>23,24</sup> and it is lower than  $r_c$  around 1.2–1.4 nm, suggesting that the extra red-shift of the emission spectra is due to the electroplex rather than exciplex.

To reveal the origin of the peaks of the spectra, we measured the EL decay curves of the Device A, as shown in Fig. 9. A prompt and a delayed component from the decay curve of Device A were clearly observed measured at 486 nm, as shown in Fig. 9. This can be attributed to the triplet-triplet annihilation (TTA) delayed fluorescence which has been found for the devices based on anthracene deviations.<sup>25</sup> From an indepth research about the EL decay curve at 486 nm, we found that there exhibit spike at 15–20  $\mu\text{s}$ , due to charge-trapping<sup>26,27</sup> existed at the interface between NPB and DPPA. As shown in Fig. 9, the spike of the curve consisted of two parts: the curve dropped quickly and then the curve rose and dropped slowly to form the tail. For the first part, it was most probably due to the fast fluorescence of DPPA which was originated from direct exciton formation on DPPA at the beginning of the electric excitation pulse, and this procedure was so fast that the curve drop quickly. Then the

electric pulse was applied, the traps for components of NPB and DPPA were filled gradually; when the electric pulse was off, the charges in the traps returned to the components of NPB and DPPA, and then at the interface between NPB and DPPA existed charge-trapping, allowing the formations of exciplex at the interface. For the decay curve measured at 662 nm, a prompt and a delayed component were also observed. The decay curves observed here may be due to the exciplex formed at the interface between NPB and DPPA.

As for the electron transport material DPPA, we also fabricated the Device B shown in Fig. 7, with the structure of on the DPPA layer which Al was directly deposited without an electron injection layer. Learned from the EL spectrum, a white emission was also obtained. Device B exhibited the CIE coordinate at (0.35, 0.36). The performance of Device A and Device B exhibited a litter lower current efficiency at 0.08 and 0.05  $\text{cd A}^{-1}$  without optimization. As reported by Chihaya Adachi,<sup>28</sup> the structures consisting of proper donor and acceptor molecules will absolutely improve the device performance from exciplex, so higher-efficiency white Device A and Device B would be obtained after optimization. Apparently, Device B showed the lower turn-on voltage than Device A by comparison shown in Fig. 10.

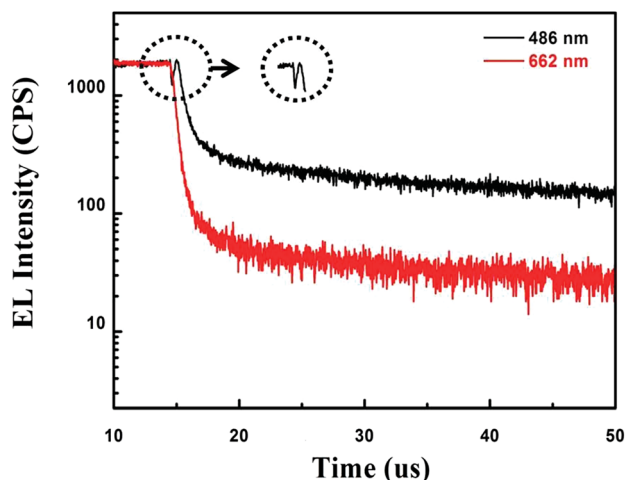


**Fig. 9** Room temperature transient EL intensity for Device A (ITO/NPB/DPPA/Mg:Ag/Ag) at different observed wavelengths (486 nm and 662 nm).

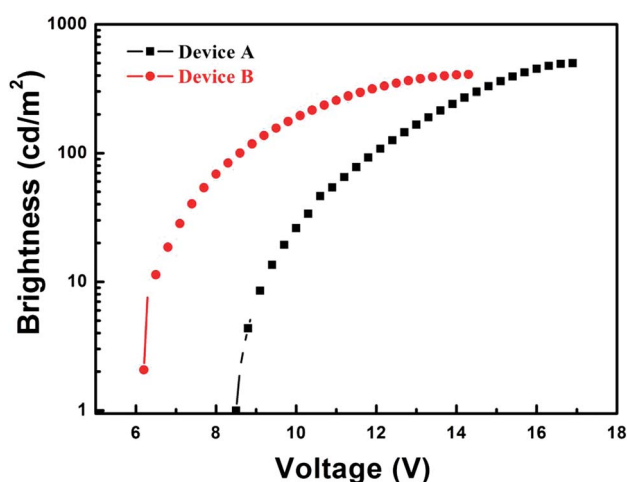


**Fig. 10** The curve of brightness–voltage for Device A (ITO/NPB/DPPA/Mg:Ag/Ag) and Device B (ITO/NPB/DPPA/Al).

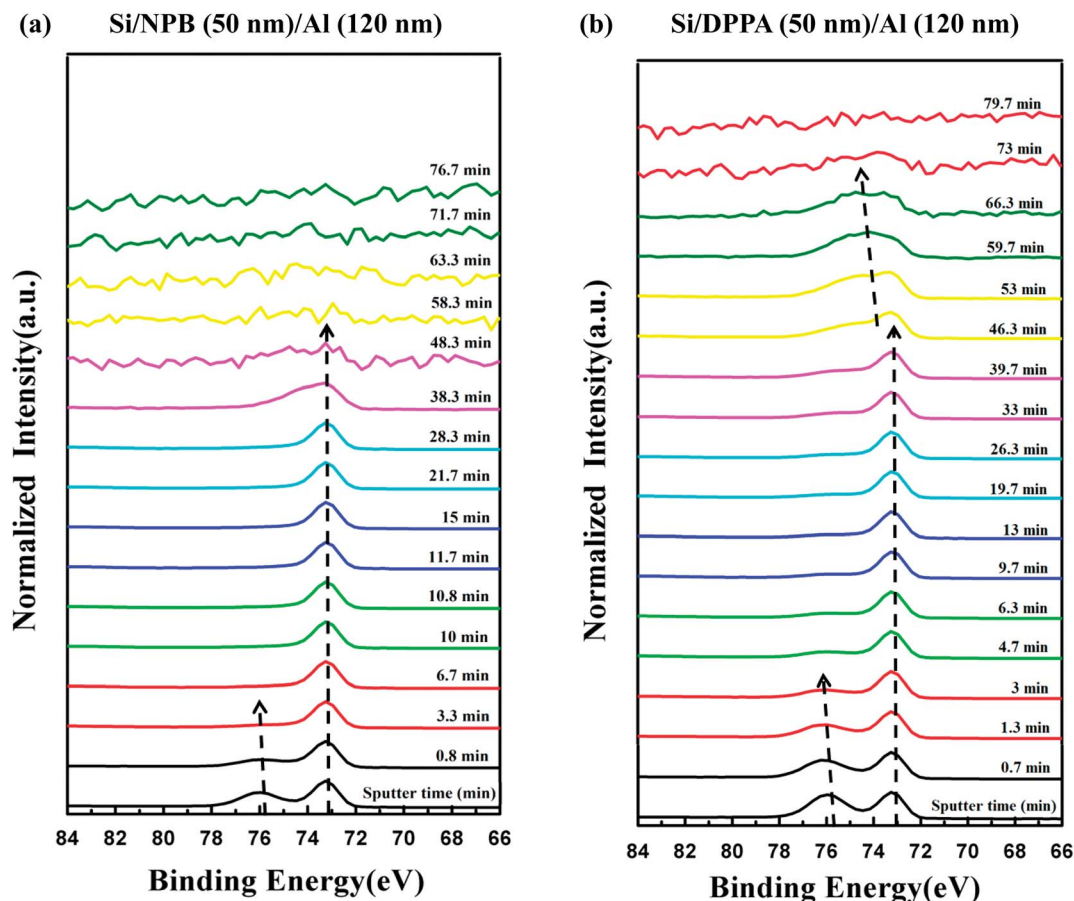


Fig. 11 (a) XPS Al<sub>2</sub>p core level spectra for the sample Si/NPB (50 nm)/Al (120 nm). (b) XPS Al<sub>2</sub>p core level spectra for the sample Si/DPPA (50 nm)/Al (120 nm).

Although the using of the electron injection layer of Mg:Ag, the OLED with high work-function Al cathode exhibited a lower turn-on voltage. This phenomenon demonstrated that the combination of DPPA and Al metal cathode indeed receives more efficient electron injection. In order to investigate the mechanism of efficient electron injection at the DPPA/Al interface, X-ray photoelectron spectroscopy (XPS) measurement was carried out to research the mechanism. 50 nm DPPA layer and 120 nm Al layer were prepared on Si substrate. For comparison, the sample Si/NPB (50 nm)/Al (120 nm) was also fabricated. The samples of Si/DPPA (50 nm)/Al (120 nm) and Si/NPB (50 nm)/Al (120 nm) were investigated *via* Ar<sup>+</sup> ion to etch the Al layer gradually.

The peaks of Al<sub>2</sub>p for the two samples with increased sputtering time are shown in Fig. 11. As shown in Fig. 11, it could be learned that the peaks of Al<sub>2</sub>p are shown at 73.0 eV and 75.8 eV from both samples' surface, respectively. This exhibition indicated that there exists metallic oxide of AlO<sub>x</sub> at initial sputter time from both samples, formed by exposed in atmosphere. As to the sample Si/NPB/Al shown in Fig. 11(a), with the increased sputtering time, the Al<sub>2</sub>p peaks of AlO<sub>x</sub> disappear gradually and the Al<sub>2</sub>p peaks of Al only existed in the sample Si/NPB/Al subsequently. This result indicated that there is no interaction at the NPB/Al interface.

For the Si/DPPA/Al sample shown in Fig. 11(b), with the sputter time increased, the spectrum of Al XPS was different from the sample Si/NPB/Al. The peak of Al<sub>2</sub>p was shifted from 73.0 eV to 75 eV during the sputter time 46.3 min to 66.3 min, indicated that there exist the strong interaction of P–O–Al at DPPA/Al interface.<sup>29,30</sup> The XPS data clearly indicated that the existence of the interaction at DPPA/Al interface is mainly the reason for efficient electron injection of DPPA/Al device.

## Conclusions

In summary, we successfully fabricated a white-OLED that the white light emission is from exciplex based on a phosphine oxide type electron transport compound in a bilayer device structure with Mg:Ag cathode and a fairly pure white emission at the equal-energy white point with CIE coordinates (0.33, 0.33) is obtained. Another white OLED with the structure without an electron injection layer, using the phosphine oxide type material DPPA layer on which Al was directly deposited, is also demonstrated. Because of the existence of interaction between the phosphine oxide group of DPPA and Al at the DPPA/Al interface, the DPPA/Al device with efficient electron injection shows the lowest turn-on voltage. These contributions can be used to simply the structure of white OLEDs.

## Acknowledgements

This research was supported by the National Natural Science Foundation of China (Grant no. 51173096, 21161160447 and 50990060) and the National Key Basic Research and Development Program of China (Grant no. 2009CB623604).

## References

- 1 J. Kido, M. Kimura and K. Nagai, Multilayer white light-emitting organic electroluminescent device, *Science*, 1995, **267**(5202), 1332–1334.
- 2 B. W. D'Andrade and S. R. Forrest, White organic light-emitting devices for solid-state lighting, *Adv. Mater.*, 2004, **16**(18), 1585–1595.
- 3 Y. Sun, N. C. Giebink, H. Kanno, B. Ma, M. E. Thompson and S. R. Forrest, Management of singlet and triplet excitons for efficient white organic light-emitting devices, *Nature*, 2006, **440**(7086), 908–912.
- 4 Z. Zhang, Q. Wang, Y. Dai, Y. Liu, L. Wang and D. Ma, High efficiency fluorescent white organic light-emitting diodes with red, green and blue separately monochromatic emission layers, *Org. Electron.*, 2009, **10**(3), 491–495.
- 5 J. Huang, W.-J. Hou, J.-H. Li, G. Li and Y. Yang, Improving the power efficiency of white light-emitting diode by doping electron transport material, *Appl. Phys. Lett.*, 2006, **89**(13), 133509.
- 6 C.-C. Chang, J.-F. Chen, S.-W. Hwang and C. H. Chen, Highly efficient white organic electroluminescent devices based on tandem architecture, *Appl. Phys. Lett.*, 2005, **87**(25), 253501.
- 7 G. Lei, L. Wang and Y. Qiu, Blue phosphorescent dye as sensitizer and emitter for white organic light-emitting diodes, *Appl. Phys. Lett.*, 2004, **85**(22), 5403.
- 8 J. X. Jiang, Y. H. Xu, W. Yang, R. Guan, Z. Q. Liu, H. Y. Zhen and Y. Cao, High-Efficiency White-Light-Emitting Devices from a Single Polymer by Mixing Singlet and Triplet Emission, *Adv. Mater.*, 2006, **18**(13), 1769–1773.
- 9 C.-I. Chao and S.-A. Chen, White light emission from exciplex in a bilayer device with two blue light-emitting polymers, *Appl. Phys. Lett.*, 1998, **73**(4), 426.
- 10 M. Zhang, Z. Chen, L. Xiao, B. Qu and Q. Gong, High-Color-Quality White Top-Emitting Organic Electroluminescent Devices Based on Both Exciton and Exciplex Emission, *Appl. Phys. Express*, 2011, **4**(8), 082105.
- 11 N. Matsumoto, M. Nishiyama and C. Adachi, Exciplex formations between tris(8-hydroxyquinolate)aluminum and hole transport materials and their photoluminescence and electroluminescence characteristics, *J. Phys. Chem. C*, 2008, **112**(20), 7735–7741.
- 12 Y. Hao, W. Meng, H. Xu, H. Wang, X. Liu and B. Xu, White organic light-emitting diodes based on a novel Zn complex with high CRI combining emission from excitons and interface-formed exciplex, *Org. Electron.*, 2011, **12**(1), 136–142.
- 13 J. Y. Li, D. Liu, C. W. Ma, O. Lengyel, C. S. Lee, C. H. Tung and S. Lee, White-light emission from a single-emitting-component organic electroluminescent device, *Adv. Mater.*, 2004, **16**(17), 1538–1541.
- 14 Z. F. Fei, N. Kocher, C. J. Mohrschladt, H. Ihmels and D. Stalke, Single crystals of the disubstituted anthracene 9,10-(Ph<sub>2</sub>P=S)(2)C<sub>14</sub>H<sub>8</sub> selectively and reversibly detect toluene by solid-state fluorescence emission, *Angew. Chem., Int. Ed.*, 2003, **42**(7), 783–787.
- 15 V. Coropceanu, J. Cornil, D. A. da Silva, Y. Olivier, R. Silbey and J. L. Bredas, Charge transport in organic semiconductors, *Chem. Rev.*, 2007, **107**(4), 926–952.
- 16 A. J. Mozer and N. S. Sariciftci, Negative electric field dependence of charge carrier drift mobility in conjugated, semiconducting polymers, *Chem. Phys. Lett.*, 2004, **389**(4–6), 438–442.
- 17 J. Li, Z. Xu, F. Zhang, S. Zhao, D. Song, H. Zhu, J. Song, Y. Wang and X. Xu, Exciplex emission of the blend film of PVK and DPVBi, *Solid-State Electron.*, 2010, **54**(4), 349–352.
- 18 D.-W. Zhao, Z. Xu, F.-J. Zhang, S.-F. Song, S.-L. Zhao, Y. Wang, G.-C. Yuan, Y.-F. Zhang and H.-H. Xu, The effect of electric field strength on exciplex emission at the interface of NPB/PBD organic light-emitting diodes, *Appl. Surf. Sci.*, 2007, **253**(8), 4025–4028.
- 19 L. Wen, F. Li, J. Xie, C. Wu, Y. Zheng, D. Chen, S. Xu, T. Guo, B. Qu, Z. Chen and Q. Gong, Exciplex emission at PVK/Bphen interface for application in white organic light-emitting diodes, *J. Lumin.*, 2011, **131**(11), 2252–2254.
- 20 F. Zhang, S. Zhao, D. Zhao, W. Jiang, Y. Li, G. Yuan, H. Zhu and Z. Xu, Exciplex emission from bi-layer blue emitting organic materials, *Phys. Scr.*, 2007, **75**(4), 407–410.
- 21 H. Zhu, Z. Xu, F. Zhang, S. Zhao and D. Song, Exciplex or exciplex emissions from the interface between aromatic diamine and 2,9-dimethyl-4,7-diphenyl-1,10-phenanthroline?, *Appl. Surf. Sci.*, 2008, **254**(17), 5511–5513.
- 22 K. Maex, M. R. Baklanov, D. Shamiryan, F. Lacopi, S. H. Brongersma and Z. S. Yanovitskaya, Low dielectric constant materials for microelectronics, *J. Appl. Phys.*, 2003, **93**(11), 8793.
- 23 M. Cocchi, D. Virgili, C. Sabatini and J. Kalinowski, Organic electroluminescence from singlet and triplet exciplexes: Exciplex electrophosphorescent diode, *Chem. Phys. Lett.*, 2006, **421**(4–6), 351–355.
- 24 J. Kalinowski, Excimers and exciplexes in organic electroluminescence, *Mater. Sci.-Pol.*, 2009, **27**(3), 735–756.
- 25 J. Wilkinson, A. H. Davis, K. Bussmann and J. P. Long, Evidence for charge-carrier mediated magnetic-field modulation of electroluminescence in organic light-emitting diodes, *Appl. Phys. Lett.*, 2005, **86**(11), 111109.
- 26 Z. Gan, R. Liu, R. Shinar and J. Shinar, Transient electroluminescence dynamics in small molecular organic light-emitting diodes, *Appl. Phys. Lett.*, 2010, **97**(11), 113301.
- 27 R. Liu, Z. Gan, R. Shinar and J. Shinar, Transient electroluminescence spikes in small molecular organic light-emitting diodes, *Phys. Rev. B: Condens. Matter Mater. Phys.*, 2011, **83**(24), 245302.

- 28 K. Goushi, K. Yoshida, K. Sato and C. Adachi, Organic light-emitting diodes employing efficient reverse intersystem crossing for triplet-to-singlet state conversion, *Nat. Photonics*, 2012, **6**(4), 253–258.
- 29 B. Zhang, C. Qin, X. Niu, Z. Xie, Y. Cheng, L. Wang and X. Li, On the origin of efficient electron injection at phosphonate-functionalized polyfluorene/aluminum interface in efficient polymer light-emitting diodes, *Appl. Phys. Lett.*, 2010, **97**(4), 043506.
- 30 S. O. Jeon, K. S. Yook, J. Y. Lee, S. M. Park, J. Won Kim, J.-H. Kim, J.-A. Hong and Y. Park, Mechanism for the direct electron injection from Al cathode to the phosphine oxide type electron transport layer, *Appl. Phys. Lett.*, 2011, **98**(7), 073306.